Aluminium to Carbon Fibre Reinforced Polymer tubes joints produced by Magnetic Pulse Welding

D. Pereira[1,2,a], J. P. Oliveira[1], T. G. Santos[1], R. M. Miranda[1], F. Lourenço[2], J. Gumpinger[3], R. Bellarosa[4]

[1] UNIDEMI, Department of Mechanical and Industrial Engineering, NOVA School of Science and Technology, NOVA University Lisbon, 2829-516 Caparica, Portugal.

[2] Omnidea, Lda, Tv. António Gedeão, 9, 3510-017 Viseu

[3] ESA/ESTEC, European Space Research and Technology Centre, Keplerlaan 1, NL-2200 AG Noordwijk, Netherlands

[4] Airbus Defence and Space Limited, Gunnels Wood Road Stevenage, SG1 2AS, United Kingdom

[a] d.pereira@campus.fct.unl.pt, corresponding author

Abstract

In this work, Aluminium AA7075-T6 to Carbon Fibre Reinforced Polymer (CFRP) tube joints using Magnetic Pulse Welding technology were performed. The process was found suitable for joining this material combination when a rigid support is used to constrain the CFRP wall displacement. A minimum discharge energy of 2.5 kJ was seen to produce tight interfaces in tubular geometry for 1 mm of stand-off distance. A larger number of turns in the coil was found to reduce both the damages caused by the impact forces and to increase the joint axial resistance. To protect the CFRP tube from impacts and achieve a weld, an electrolytic Nickel coating was deposited over the CFRP tube. Welding was produced between the coating and the aluminium tube with no intermetallic compounds observed on the interface for the energies tested.

Keywords: Metal to non-metal joining; Magnetic Pulse Welding; AA7075-T6; Carbon Fibre Reinforced Polymer (CFRP); Overlap tubular joints; Mechanical testing.

Graphical Abstract

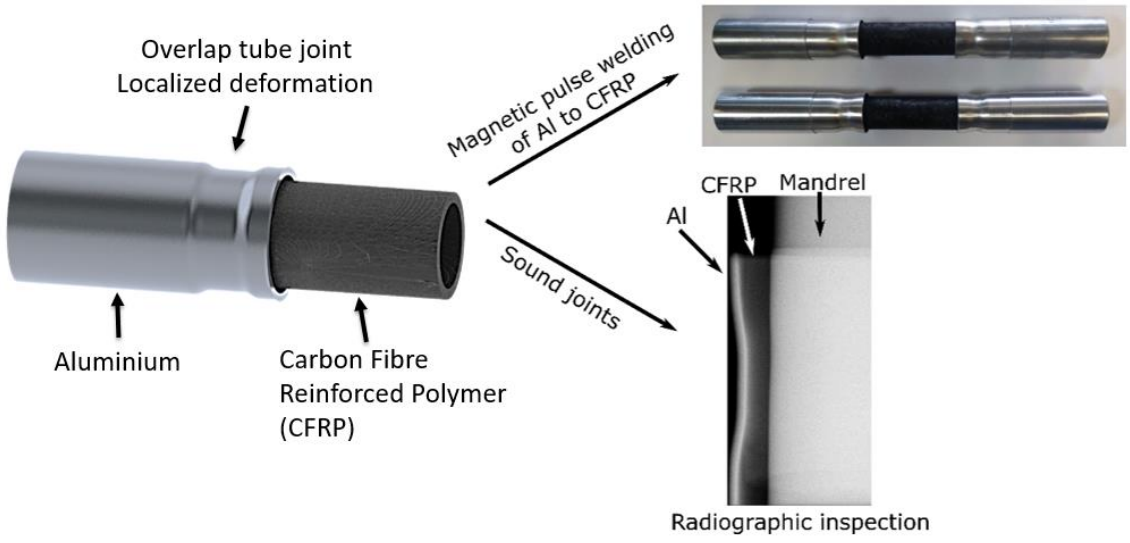

Research Highlights

- AA7075-T6 to Carbon Fibre Reinforced Polymer (CFRP) tubular joints in overlap configuration were produced by magnetic pulse welding;
- Parameter tuning and effects on the CFRP tubes integrity was studied;
- Full perimeter contact for 2.5 kJ of discharge energy;
- Welding achieved between the aluminium flyer and the electrolytic Nickel coating deposited over the CFRP tube.

1. Introduction

Solid state joining processes are attracting increased interest due to the possibility to produce multi-material hybrid structures, since the material reactions involved in melting and solidification are avoided, using tuned parameters, allowing homogenous and dissimilar joining regions with superior properties [1]. Among the different solid-state techniques, Magnetic Pulse Welding (MPW) technology aroused interest due to its great capabilities in producing overlapped joints, both planar and tubular, with little or even no thermal affected regions [2].

MPW is currently used to perform similar [3] and dissimilar [4] metallic joints in difficult to weld metals, such as Al, Cu and Ni, due to the differences in the thermo-physical properties. However, when there is a need to join metals to composite materials, specially polymer-based ones, not all welding techniques can be used. For example, fusion-based welding of polymeric composites requires tight control of the welding parameters [5,6], which often is not suitable for large scale production. To overcome such difficulty solid-state welding techniques can be used [7,8]. Among the several existing solid-state techniques, MPW technique is a viable way to obtain metal to non-metals combinations. Similar to other impact welding processes, such as explosive welding, in MPW it is possible to control the discharge energy, as well as, the stand-off distance, which is the distance the flyer material has to accelerate, and the impact angle [9].

Watanabe et al. in [10] studied the production of joints via MPW in aluminium to metallic glass and showed the need to carefully control the impact force in this combination. Since these materials tend to present highly dissimilar behaviours, the impact can produce defects or even damage the target if not properly controlled. In this case, the brittle behaviour of the metallic glass required the use of a shock absorbent plate, made from annealed aluminium.

The need to control the impact force and, therefore, the discharge energy, is even more noticeable when the materials to be joined are damaged upon impact. Aizawa et al. studied the production of flexible printed circuit boards (FPCB) in which MPW was used as driving force to promote the adhesion between the polyamides [11]. Since the flyer material did not present a good surface conductivity, a driver plate made of aluminium was used to push the flyer against the target. The wavy interface typical of impact welding processes [12] was only observed when the driver plate was used. When the driver was not used, although joining was achieved, no evident wavy interface was detected.

In this study aluminium to carbon fibre reinforced polymer tubular joints were produced by magnetic pulse welding. The aim was to produce structural joints using a solid-state joining technique. A systematic analysis of the welding parameters and their effect of the produced joints was performed.

The microstructure, defects and mechanical properties were studied via optical and electron microscopy, non-destructive testing and tensile testing, respectively. Due to the significantly different material's properties, the joint is created due to mechanical interlocking upon high speed impact. The axial resistance was determined and correlated with the joint features. Successful joining of this dissimilar combinations opens new possibilities for application in the aerospace field.

The effect of the coil length on the final result was studied since, if no mechanical interlocking is achieved, which normally produces a wavy interface, the axial resistance will be only due to Coulomb friction between both materials. It is known that this force depends on the contact force and on the friction coefficient, thus the contact area should not be a parameter. However, changing the contact area will cause a variation in the contact force and, since the coil length depends on the number of coil turns, the produced magnetic pressure is affected by the coil length and thus the deformation force changes for constant discharge energy.

2. Materials and methods

In this study joints of aluminium alloy AA7075-T651 tubes to Carbon Fibre Reinforced Polymer tubes, were produced via magnetic pulse welding. The goal of this paper to test the feasibility of producing structural joints between these materials without using adhesives. Only a mechanical joint is produced, rather than an actual weld, since this is cannot be achieved directly between these two materials. Therefore, the joints are not welded but crimped.

The material used to produce the CFRP tubes was Torayca T300 fibre fabric. The CFRP tubes were the target and had an outer diameter of 20 mm and a wall thickness of 2 mm. The flyer tube was machined from a rod with an outer diameter of 25 mm and with a wall thicknesses of 1 mm.

The developed MPW prototype machine used to produce the joints is the same used in the previous tests [13]. The equipment has an architecture similar to most commercially available machines. However, it was optimized to reduce the discharge energy, thus improving the overall machine efficiency.

Several parameters were tested and optimized to achieve joining. These were: the discharge energy, E [J]; the stand-off distance, r [mm]; and the impact angle, θ [º]. The range used for each parameter is depicted in Table 1. The presented energies are the output discharge at the coil contacts.

Table 1 – Range of process parameters tested.

Process parameter	Range tested
Discharge Energy, E [kJ]	1 to 3.5 (0.5 increments)
Stand-off distance, r [mm]	0.5, 1.0 and 1.5
Impact Angle, θ [º]	5 to 20

The number of turns in the coils was of 6, 8 and 10 turns which, combined with the stand-off distance, gives the geometrically imposed impact angle. The coil wire diameter was of 1 mm and the turns were wrapped tight without a gap. As a result, the coil height is given by the number of turns and the overlap changes with the coil position as presented in [13]. The Impact angle is calculated as presented in Figure 1.

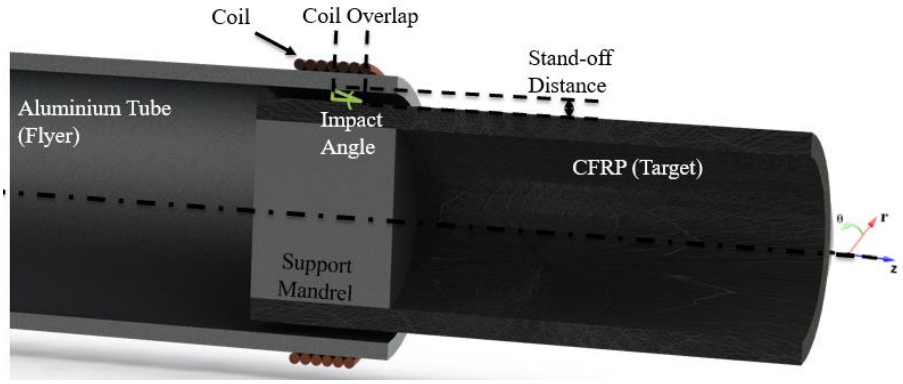

Figure 1 – Joint schematic: Geometrical parameters definition

To evaluate the joints integrity, X-ray inspections were made to identify possible damages induced into the CFRP tubes and these were complemented with optical observations and scanning electron microscopy (SEM) of the cross-sections to verify the contact between both parts. Radiographic analysis was performed using a combination of a KODAK 2100 RX unit and a KODAK RVG 5100 digital radiographic system. The X-ray unit is a high frequency DC X-ray generator with a tube voltage of 60 kV working at 7 mA with a 23×35 mm collimator. This system features a spatial resolution of 18:5 µm, an active sensor area of 22×30 mm and a maximum integration time of 620 ms. The samples were also cross sectioned transverse to the tube's axis and mechanically polished for optical and scanning electron microscopy.

Hardness profiles were measured on the observed sections using a Mitutoyo HM-112 Micro-Vickers Hardness Testing Machine using a load of 2.94 N with a dwell time of 10 second. Each indentation was spaced 200 µm from the following one.

The joint axial resistance was evaluated by uniaxial tensile tests performed using an Instron tensile testing machine with a cross-head displacement speed of 5 mm/min. No strain gauge could be used since it would be attached to different diameters. This would impose a tilt angle to the strain gauge which would create a multidirectional solicitation. Since no weld is produced and both parts are crimped the resistance-section cannot be defined thus, the resistance profiles are presented as force-displacement profiles.

3. Results and discussion

3.1. Process optimization

Preliminary tests using a stand-off distance of 1 mm, a discharge energy of 1 kJ and a coil with 6 turns, revealed that failure of the CFRP tubes occurred, as depicted in Figure 2. Discharge energies below 1 kJ could be used. However, there is not enough deformation of the aluminium flyer to produce a joint. Therefore, to avoid the massive damage on the CFRP tubes due to the impact, a mandrel was used to provide additional support to the CFRP tubes. Three distinct materials (HDPE, epoxy resin and aluminium) were selected to evaluate their effectiveness as mandrels in this dissimilar joint. The selection of these potential candidates was based on their stiffness. The mandrels were cylinders machined tight to the CFRP tube inner diameter to constrain the CFRP tube wall movement.

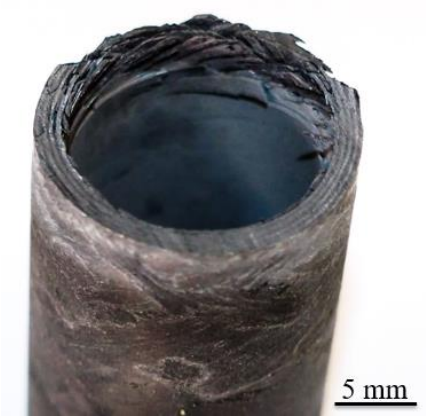

Figure 2 – Sample G1 after cross sectioning.

In accordance with the processing parameters depicted in Table 1, several parameter combinations were tested and investigated, varying one parameter at the time, to fully understand the effect of each one on the produced joints. Samples were evaluated using X-ray inspections and optical microscopy observations of the transverse sections. The parameters combinations tested along with the support mandrel used, are presented in Table 2. The flyer thickness was kept constant, at 1 mm, for these tests. The samples reference is not continuous due to repetition of some test conditions. The lower discharge energies and stand-off distances were not tested for all supports since they either had lack of joint resistance or excessive damage was caused to the CFRP tubes. Furthermore, the larger discharge energies were only tested with the aluminium supports due to its higher stiffness. The more ductile mandrel materials allow more deformation of the CFRP tube causing it to crack.

148 ***Table 2 – Samples tested and their processing parameters.***

Sample Reference			Stand-off Distance	Discharge Energy	Nº of Coil Turns	Impact Angle
H	R	A	[mm]	[kJ]		[º]
G2	G3	-	1.0	1.0	6	17.4
G4	G13	-	1.0	2.0	6	17.4
G9	G16	-	1.0	2.0	8	13.1
G24	G20	-	0.5	2.5	6	8.9
G22	G19	G27	0.5	2.5	8	6.6
G25	-	-	0.5	2.5	10	5.3
G7	G15	G30	1.0	2.5	6	17.4
G11	G17	G31	1.0	2.5	8	13.1
G28	G26	G29	1.5	2.5	8	19.2
G23	G21	-	0.5	3.0	8	6.6
G8	G14	G34	1.0	3.0	6	17.4
-	-	G35	1.0	3.0	8	13.1
-	-	G41	1.0	3.0	6	17.4
-	-	G47	1.0	3.5	10	10.5

149 Note: H, R and A refer to the mandrels materials: HDPE (H), Epoxy resin (R) and Aluminium (A).

150 X-ray radiography was performed on the samples to evaluate the presence of defects. In the following X-
151 ray images, the brighter stripe corresponds to the aluminium and the adjacent marked tenuous stripe is
152 the CFRP tube wall. The tube axis is marked with a dash dot line.

153 Varying the stand-off distance for a constant discharge energy yields different contact areas and force
154 since the plastic deformation imposed to the flyer is constant. As observed in Figure 3, the maximum
155 deformation on the aluminium is controlled by the discharge energy thus, smaller stand-off distances
156 impose larger deformations on the CFRP tubes and tend to crack the CFRP material upon impact. These
157 samples highlighted the need for a stiff mandrel since the discharge pulse has the same duration,
158 accelerating the aluminium to the same velocity. Therefore, the magnetic field is still pushing the
159 aluminium forward after impacting the CFRP tube causing it to crack without a sound support.

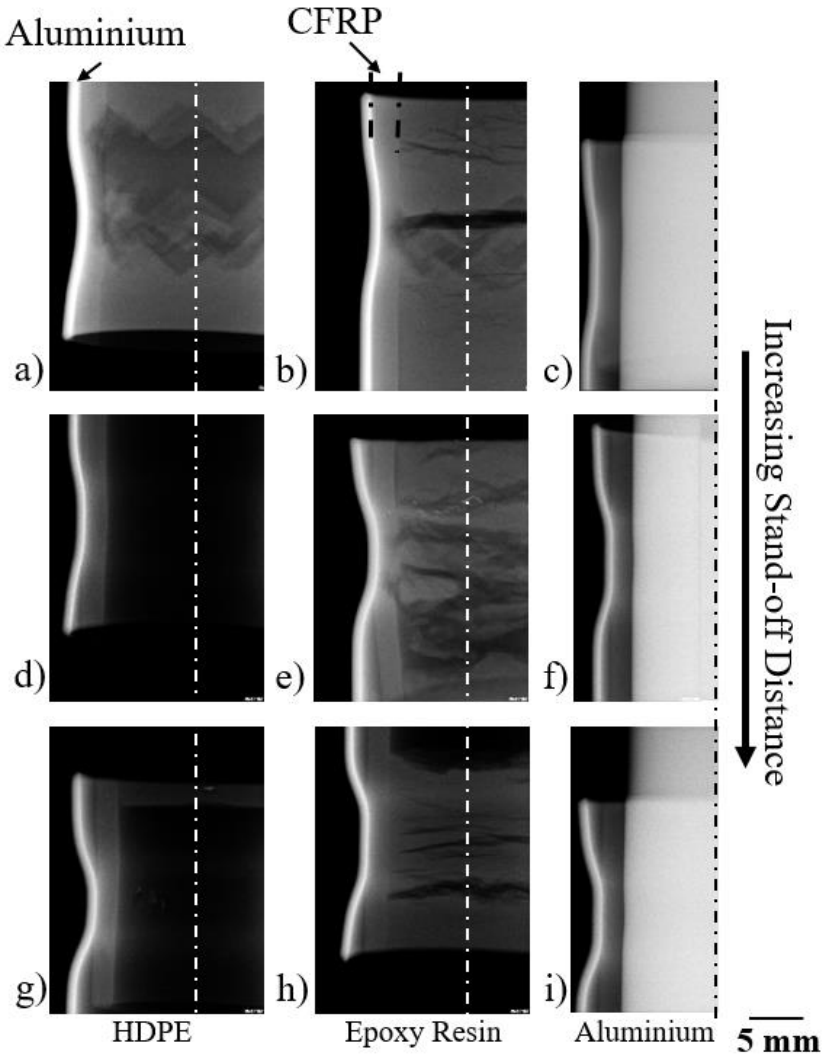

Figure 3 – Radiographic images of joints produced with: discharge energy of 2.5 kJ an 8-turn coil and varying the stand-off distance. Mandrel type: HDPE (details a)G22; d)G11 and g)G28); Epoxy Resin (details b)G19; e)G17 and h)G26); Aluminium (details c)G27; f)G31 and i)G29).

Increasing the discharge energy for constant stand-off distances and number of turns in the coil has similar effects, especially for the more ductile mandrels which allow the CFRP tube to deform. This is due to the magnetic pressure produced which is directly proportional to the discharge current and, thus, the discharge energy.

As depicted in Figure 4, if no cracks are produced due to impact, larger discharge energies produce larger contact areas between both parts. However, if excessive discharge energy is used, the composite can be damaged due to excessive deformation beyond the elastic limit, leading to the crack initiation and propagation, since there is no internal support.

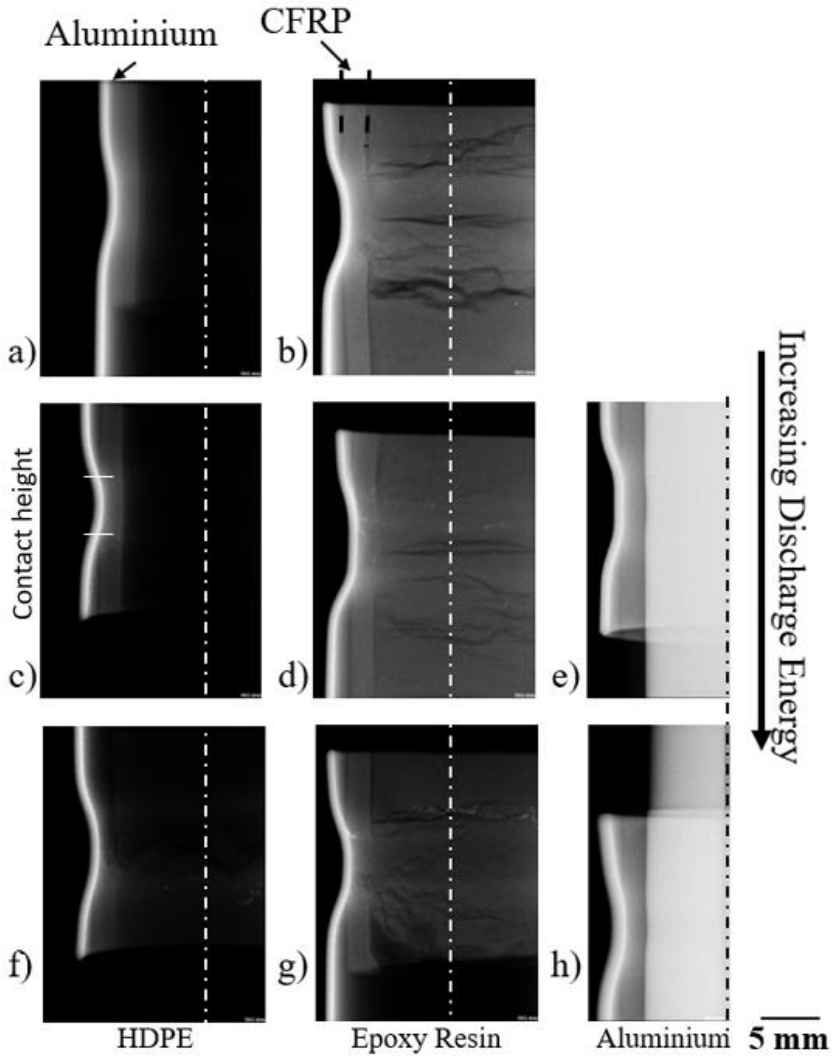

Figure 4 – Radiographic images of joints produced with: stand-off distance of 1 mm, a 6-turn coil and varying discharge energy. Mandrel type: HDPE (details a)G4; c)G7 and f)G8); Epoxy Resin (details b)G13; d)G15 and g)G14); Aluminium (details e)G30 and h)G34).

A discharge energy of 2.5 kJ was identified as the minimum energy to ensure full perimeter contact between both materials. However, the use of the aluminium mandrel is mandatory to constrain the CFRP wall deformation. Using a discharge energy of 3 kJ, for the same support, produced a larger contact along the joint axis which is important to improve the concentricity between both parts and allow a more even pressure distribution.

Discharge energies below 2 kJ resulted in loose parts or joints with low axial resistance, while excessive discharge energy produced larger deformations on the CFRP tube causing it to crack. The heat input due to Joule effect appears to be reduced since no evidence of high temperature damages were seen in the observations. Nevertheless, and as highlighted in Figure 4, if the mandrel fully constrains the CFP tube wall, preventing large deformations on the CFRP tube, cracks are avoided even for discharge energies up to 3 kJ.

As shown in Figure 4 and Figure 5, larger impact angles reduce damage on the CFRP tubes since, either the stand-off distance increases, which reduces the impact velocity as shown before, or the number of turns in the coil increases which produces a larger impact area, thus reducing the impact force. Nevertheless, the support mandrel stiffness is a key characteristic to avoid cracks due to impact on the CFRP tubes as proved by the samples produced with the aluminium mandrel.

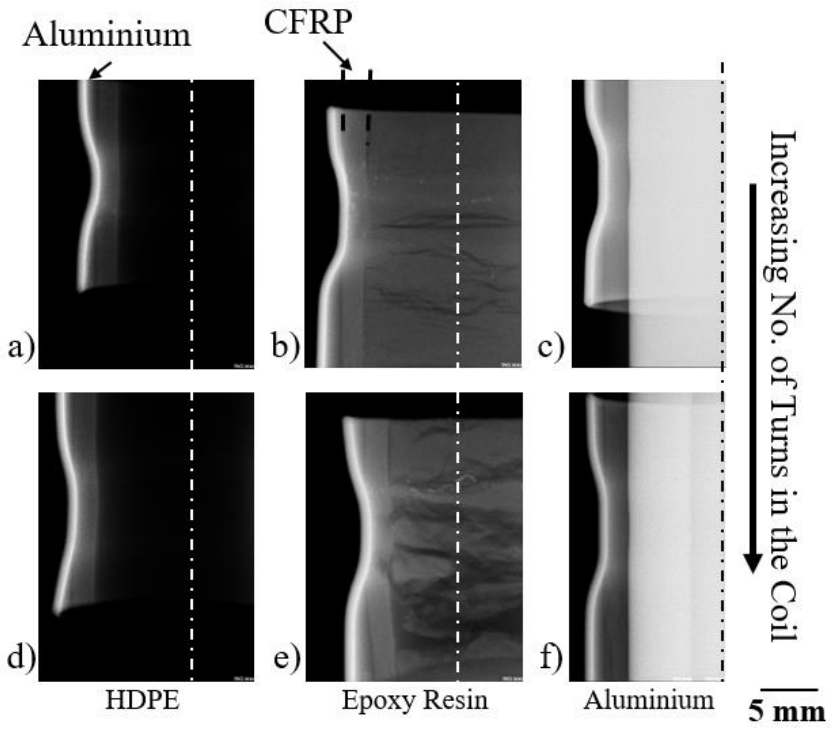

Figure 5 – Radiographic images of joints produced with: stand-off distance of 1 mm, discharge energy of 2.5 kJ and varying number of turns in the coil. Mandrel type: HDPE (details a)G7 and d)G11); Epoxy Resin (details b)G15 and e)G17); Aluminium (details c)G30 and f)G31).

Regarding the discharge energy it was found that to ensure continuous contact along the perimeter a minimum energy of 2.5 kJ had to be used. However, with the proper selection of the support, as the aluminium rod, a discharge energy of 3 kJ led to the best results since the contact length between both parts was more homogenous. Higher energies produce larger deformations which in turn cause damage to the CFRP tubes. Nonetheless, if proper support is used, and the CFRP tube wall movement is constrained, this damage can be avoided, even for high discharge energies.

As identified by the X-ray radiographs, when the impact force is excessive, either by using insufficient stand-off distance or excessive discharger energy, the CFRP tubes crack. This is due to its brittle behaviour which, combined with lack of stiffness of the support mandrel, initiate cracks on the inner surface which propagate along the thickness to the outer surface, as seen in Figure 6. These finding were also confirmed for less stiff supports and coils with few turns.

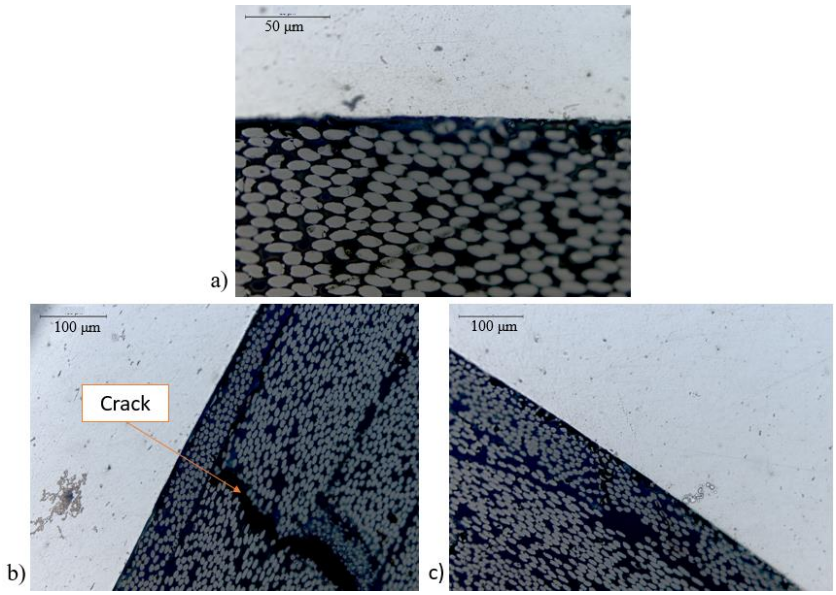

Figure 6 – Interface details of sample G7 (DE=2.5 kJ; SD=1 mm; 6-turn coil with HDPE mandrel).

The cracks observed were radial which, for larger impact forces, could progress through the full thickness of the CFRP tube. When these two types of damages were observed together, catastrophic failure of the CFRP tube wall was visible, as shown in Figure 7, where a large fraction detached during the polishing stage due to the severe damages observed. In this case, despite the lack of support, the damage is more localized on the left side of the cross section due to misalignment of both parts when positioning prior to joining.

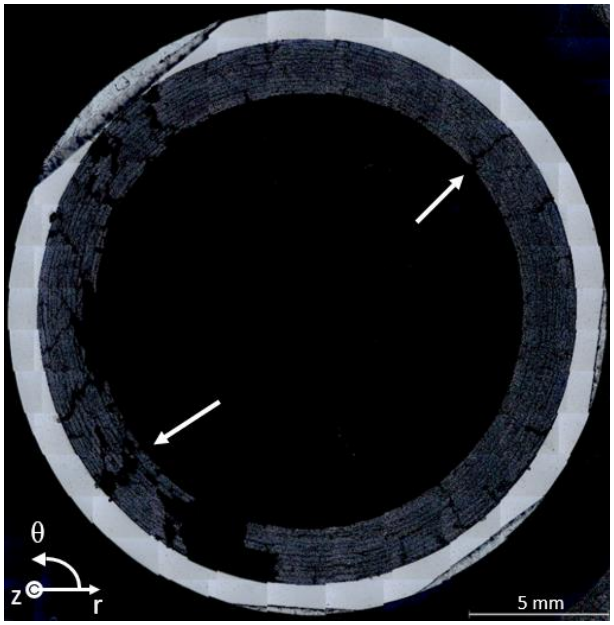

Figure 7 – Cross section macrograph of specimen G17. The arrows indicate the location of the cracks formed.

As identified by X-rays, when using an aluminium mandrel, crack propagation was prevented, even when the same discharge energy was used (sample G17 in Figure 8), since the CFRP tube wall movement was

severely constrained. Cracks could be completely avoided with a fine tuning of the process parameters and a tight support to fully constrain the CFRP wall movement which also increased the contact area between both parts, producing an interface with less gaps between both parts along the perimeter, as shown in Figure 9.

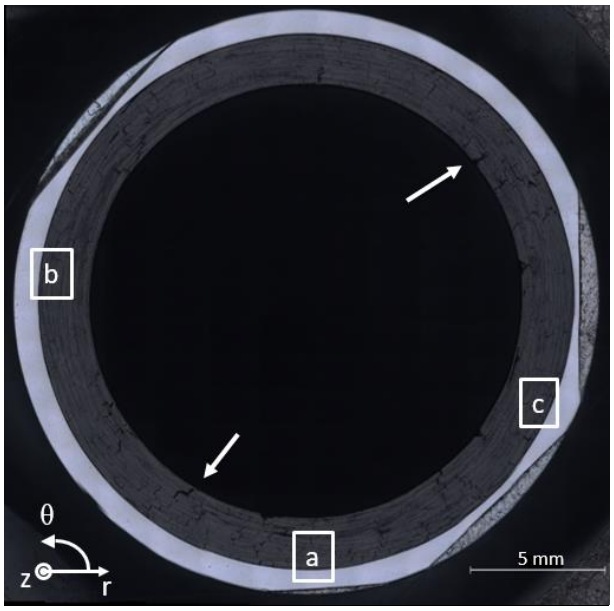

Figure 8 – Cross section view of sample G31 (DE=2.5 kJ; SD=1 mm; 8-turn coil with aluminium support mandrel). The arrows indicate the location of the cracks formed.

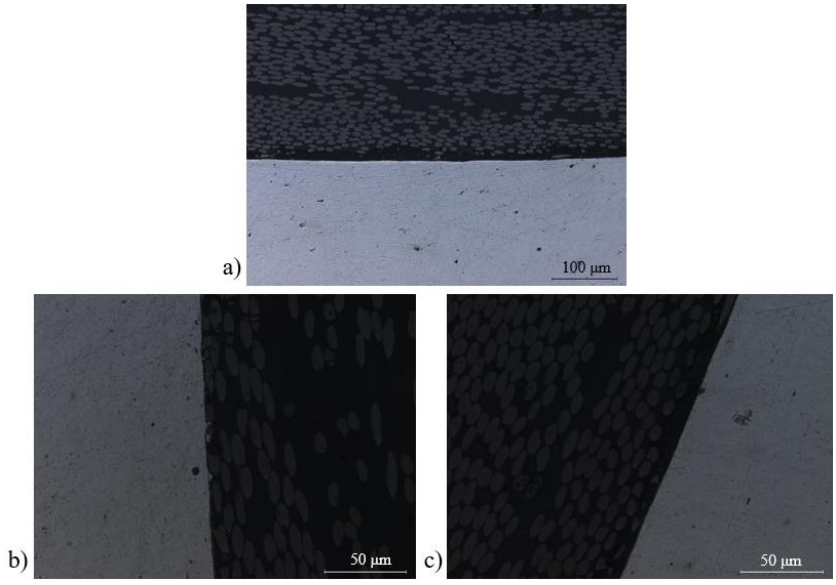

Figure 9 – Micrographs of sample G31 (DE=2.5 kJ; SD=1 mm; 8-turn coil with aluminium support mandrel) in the regions highlighted in Figure 8; a), b) and c) respectively.

When using a support mandrel, machined tight to the inner diameter of the CFRP tube, completely constraining the wall deformation, no damage from the MPW process is visible.

The close-fitting interfaces were confirmed under SEM observations, depicted in Figure 10, where the aluminium slightly penetrates the resin contouring the carbon fibre filaments, in a mechanical locking mechanism.

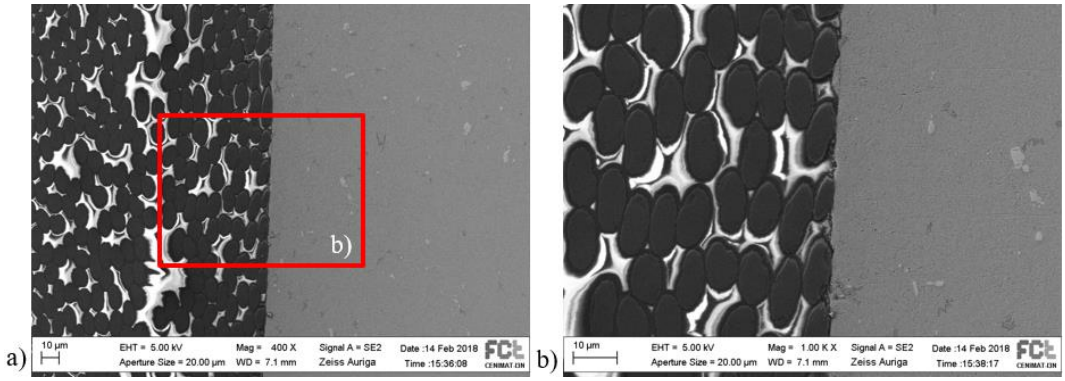

Figure 10 – SEM image of the aluminium to CFRP interface of specimen G35 (discharge energy of 3 kJ; stand-off distance of 1 mm; 8-turn coil with aluminium support mandrel)

For this materials combination, the impact angle is not a key parameter since no weld is produced and thus jetting, and its cleaning effect is of reduced importance. However, the impact angle is important for the impact propagation in order to achieve a tight fit between both parts, as presented in the SEM images, with a wavy interface to produce mechanical locking, thus increasing the axial resistance.

3.2. Joint axial resistance

Tensile tests were performed to establish a minimum resistance of the joint specimens. The specimens tested were produced using a 10-turn coil at tube centre, 3 kJ of discharge energy and 1 mm of stand-off distance. The specimens only had one aluminium fitting to test accurately the joint strength.

A mandrel was machined tight to the CFRP tube inner diameter to provide support both to produce the joint and to fix the carbon fibre part to the tensile test machine. Regarding the aluminium part a piece from a solid round bar was used to have a solid basis to fix to the testing machine while the other side was machined to a tube with 25 mm outer diameter and 1.5 mm of wall thickness to produce the joints. The tensile test setup is presented in Figure 11.

Figure 11 – Tensile testing setup

A non-sliding criterion was imposed thus, the resistant force considered is the maximum before the sample parts start sliding. The joint behaviour is presented in Figure 12 with the failing point marked with an arrow.

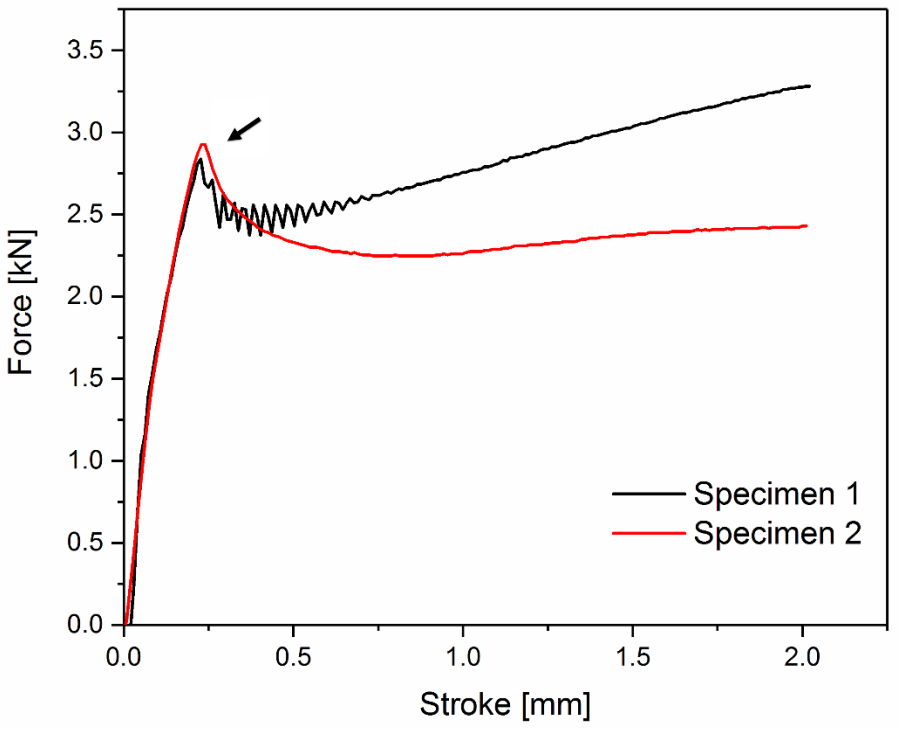

Figure 12 – Typical force-stroke curves for two different samples.

As observed, the two specimens tested presented similar behaviour in the elastic regime achieving a peak load of 2.9 kN, before sliding occur. The minimum force to slide is similar for both specimens which shows consistent results for the contact established with the tested conditions. However, after sliding initiation the behaviour can be quite different. These differences on the resistance profile are due to different precision on the mandrel diameter which influences the contact along the tube axis after starting to slide, which is in good agreement with the need to use stiff mandrels to ensure homogenous contact on the joint. Specimen 1 had a tighter mandrel resulting in the ripple effect typical of sliding and the resistance increment is also due to the jetting which is deposited on the adjacent region of the joint, acting as a barrier to sliding owed to the tight fit between both parts.

These mechanical results are promising since the joint resistance comes from the mechanical locking and the friction between both parts which directly correlates with tube dimensions.

As expected, and as shown in Figure 13, failure of the tensile test specimens occurred at the joint interface since no weld or chemical bond is produced. The aluminium adhesive tape visible on one side of the CFRP tube was used to avoid damage to the fibres when positioning the specimen on the tensile machine.

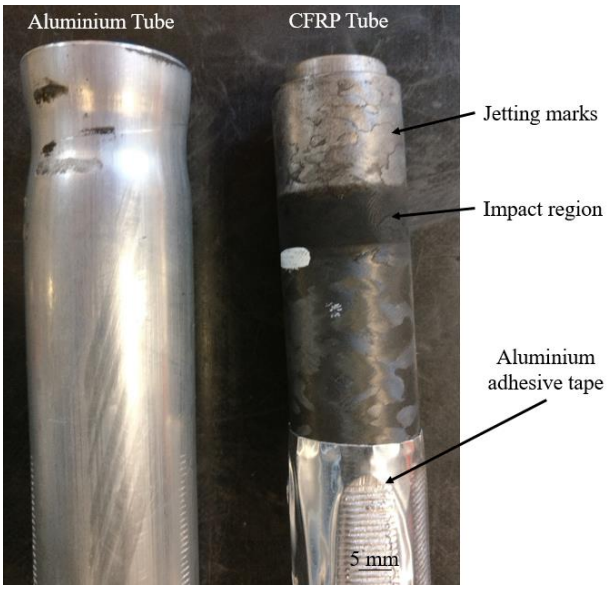

Figure 13 – CFRP tube specimen pull out after crimping.

To avoid damage on the CFRP tube and increase the joint mechanical resistance the use of a ductile metallic coating to absorb part of the deformation and to promote welding between the coating and the aluminium tube can be considered.

To test the coating hypothesis, an electrolytic coating of Nickel was deposited over the CFRP tube. For these tests, the aluminium tube thickness was kept at 1 mm, the coating thickness was of 80 µm and the welding parameters used were a discharge energy of 3 kJ, stand-off distance of 1 mm and 6-turn coil, using an aluminium mandrel. No damage was observed on the joint cross-section, showing that part of the energy is now used to weld and to deform the coating thus, less energy will be transferred to deform the CFRP tube.

No compounds at the nickel/aluminium interface was observed showing that no liquid phase was present due to the low energy transferred contrary to other studies where Ni-Al binary phases in the form of an amorphous alloy were observed at the interface due to melting and rapid solidification of both materials [14].

Welding between the aluminium tube and the nickel coating was confirmed under SEM and via energy dispersive spectroscopy (EDS) inspections. As depicted in Figure 14, nickel has good adhesion to the CFRP tube. Between the aluminium and the coating, a tight interface was achieved with almost a full perimeter.

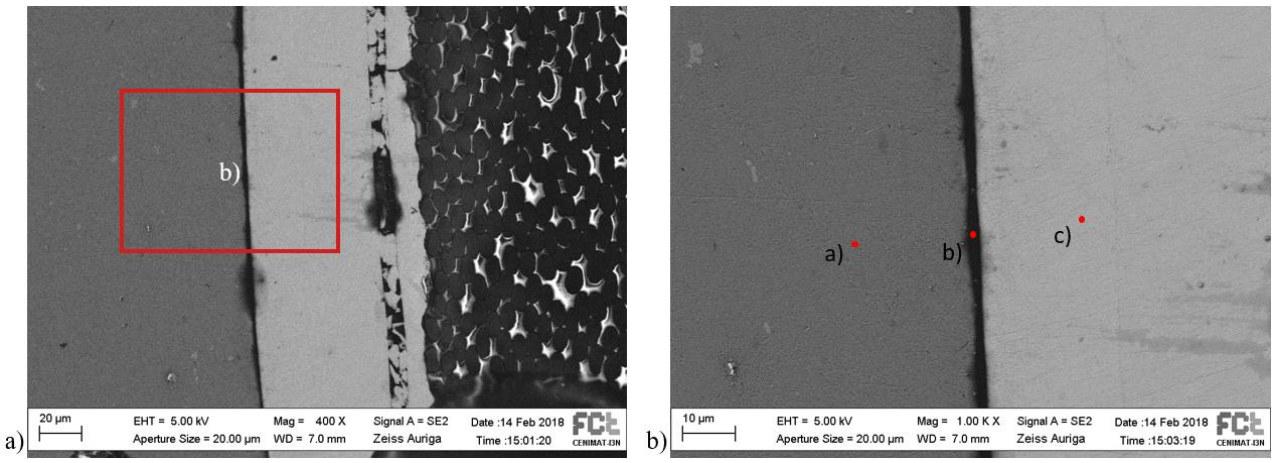

Figure 14 – SEM image of the interface of specimen G40 Welding parameters: discharge energy of 3 kJ; stand-off distance 1 mm; 6-turn coil and aluminium mandrel. The red spots in Figure 14 b) mark the regions were EDS measurements were performed. EDS results are presented in Figure 15.

The black line of Figure 14 is a shadow effect between both materials since as inferred from the EDS measurements presented in Figure 15, there is material in that region, mostly from the coating but also aluminium. Therefore, joining was observed between the nickel coating and the aluminium flyer.

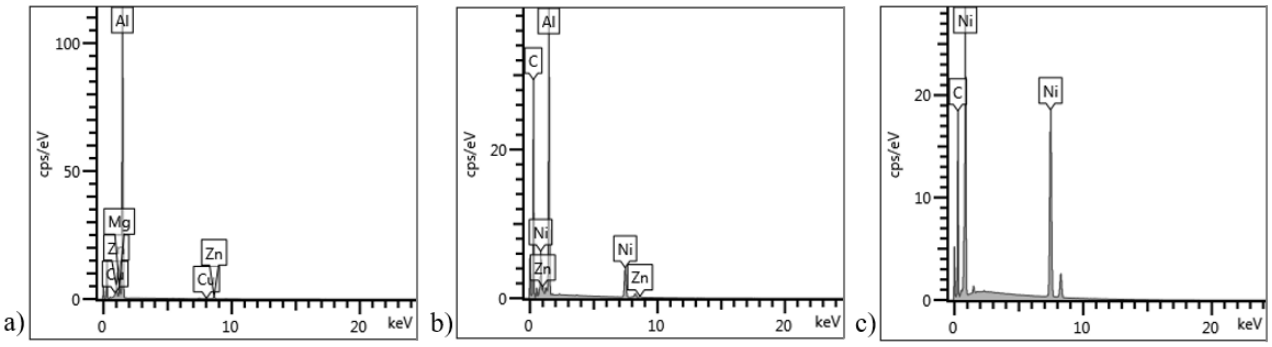

Figure 15 – EDS profiles at the nickel aluminium/interface of specimen G40 Welding parameters: DE=3 kJ; SD=1 mm; 6-turn coil and aluminium mandrel.

The weld with the coating avoided cracking of aluminium since part of the energy is absorbed by it and thus it is not stored as elastic deformation on the CFRP tube. Additionally, it also increases the resistant section of the joint by adding thickness and homogenizes the contact force distribution on the aluminium tube. Due to the good adhesion with the substrate, the expanding force is more evenly distributed. However, it should be combined with a larger wall thickness on the aluminium tube to ensure that the aluminium cracks are completely avoided.

Jetting, which was observed in Figure 13, was confirmed with EDS analysis as shown in Figure 16, where aluminium traces were found attached to the CFRP tube outer wall on the section adjacent to the impact zone (marked in the previous figure). On detail d), two large aluminium fragments are visible but also scattered particles on the CFRP surface projected from the jetting.

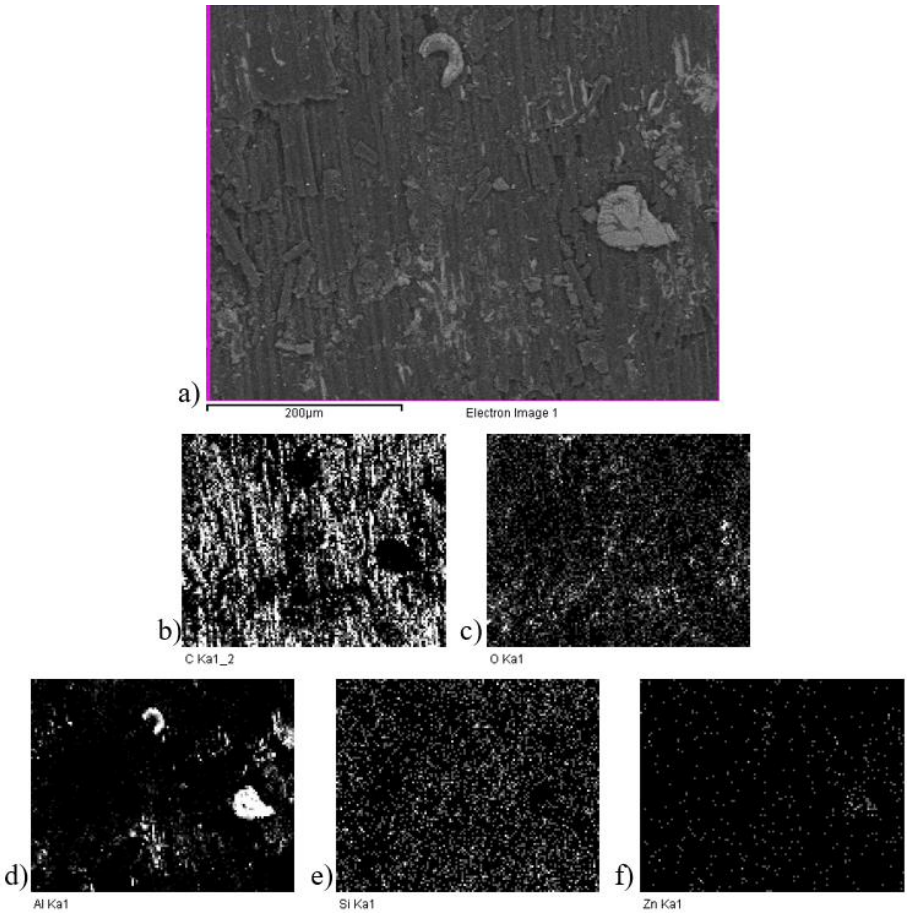

Figure 16 – EDS analysis of the CFRP outer surface near the impact zone a). Elemental dispersion b) C; c) O; d) Al; e) Si; f) Zn.

The presence of jetting without damaging the CFRP tube is relevant when using metallic coatings since it is mandatory to ensure that the surfaces are clean and prepared for the welding process.

4. Conclusions

In this work, production of aluminium to carbon fibre tubes joints was possible using a magnetic pulse welding machine. The following main conclusions were drawn:

- Aluminium to Carbon Fibre Reinforced Polymer (CFRP) tubes joints were successfully produced by Magnetic Pulse Welding process.
- A minimum of 2.5 kJ of discharge energy is required to ensure a good fit and sound contact between both counter-parts with a stand-off distance of 1 mm.
- The use of a stiff mandrel is mandatory to constrain the CFRP tube wall to avoid damage.
- The maximum axial load achieved before sliding was of 2.9 kN and good reproducibility was obtained.
- Ductile metallic coatings can be used to absorb part of the energy to avoid damage on the CFRP tube.

Acknowledgements

DP and FL acknowledge Project SpIM, (2016/10605), supported by Fundo Europeu de Desenvolvimento Regional (FEDER), Programa Operacional Regional do Centro and Portugal2020, as well as, project funded by ESA (ESA contract 4000111471/14/NL/PA). RMM, TGS and JPO acknowledge Fundação para a Ciência e Tecnologia (FCT) for its financial support via the project UID/EMS/00667/2019.

Data Availability

The raw and processed data required to reproduce these findings cannot be shared at this time as the data also forms part of an ongoing study.

References

[1] J.P. Oliveira, J.F. Duarte, P. Inácio, N. Schell, R.M. Miranda, T.G. Santos, Production of Al/NiTi composites by friction stir welding assisted by electrical current, Mater. Des. 113 (2017) 311–318. doi:10.1016/j.matdes.2016.10.038.

[2] A. Kapil, A. Sharma, Magnetic pulse welding: an efficient and environmentally friendly multi-material joining technique, J. Clean. Prod. 100 (2015) 35–58. doi:10.1016/j.jclepro.2015.03.042.

[3] A. Stern, M. Aizenshtein, Bonding zone formation in magnetic pulse welds, Sci. Technol. Weld. Join. 7 (2002) 339–342. doi:10.1179/136217102225002673.

[4] Z. Xu, J. Cui, H. Yu, C. Li, Research on the impact velocity of magnetic impulse welding of pipe fitting, Mater. Des. 49 (2013) 736–745. doi:10.1016/j.matdes.2012.12.059.

[5] A. Yousefpour, M. Hojjati, J.-P. Immarigeon, Fusion Bonding/Welding of Thermoplastic Composites, J. Thermoplast. Compos. Mater. 17 (2004) 303–341. doi:10.1177/0892705704045187.

[6] B. Cosson, M. Deléglise, W. Knapp, Numerical analysis of thermoplastic composites laser welding using ray tracing method, Compos. Part B Eng. 68 (2015) 85–91. doi:10.1016/j.compositesb.2014.08.028.

[7] R. Kumar, R. Singh, I.P.S. Ahuja, R. Penna, L. Feo, Weldability of thermoplastic materials for friction stir welding- A state of art review and future applications, Compos. Part B Eng. 137 (2018) 1–15. doi:10.1016/j.compositesb.2017.10.039.

[8] F. Lionetto, C. Mele, P. Leo, S. D'Ostuni, F. Balle, A. Maffezzoli, Ultrasonic spot welding of carbon fiber reinforced epoxy composites to aluminum: mechanical and electrochemical characterization, Compos. Part B Eng. 144 (2018) 134–142. doi:10.1016/j.compositesb.2018.02.026.

[9] M. Hahn, C. Weddeling, J. Lueg-Althoff, A.E. Tekkaya, Analytical approach for magnetic pulse welding of sheet connections, J. Mater. Process. Technol. 230 (2016) 131–142. doi:10.1016/j.jmatprotec.2015.11.021.

[10] M. Watanabe, S. Kumai, G. Hagimoto, Q. Zhang, K. Nakayama, Interfacial Microstructure of Aluminum/Metallic Glass Lap Joints Fabricated by Magnetic Pulse Welding, Mater. Trans. 50 (2009) 1279–1285. doi:10.2320/matertrans.ME200835.

[11] T. Aizawa, K. Okagawa, M. Kashani, Application of magnetic pulse welding technique for flexible

printed circuit boards (FPCB) lap joints, J. Mater. Process. Technol. 213 (2013) 1095–1102. doi:10.1016/j.jmatprotec.2012.12.004.

[12] S. Patra, K.S. Arora, M. Shome, S. Bysakh, Interface characteristics and performance of magnetic pulse welded copper-Steel tubes, J. Mater. Process. Technol. 245 (2017) 278–286. doi:10.1016/j.jmatprotec.2017.03.001.

[13] D. Pereira, J.P. Oliveira, T. Pardal, R.M. Miranda, T.G. Santos, Magnetic pulse welding: machine optimisation for aluminium tubular joints production, Sci. Technol. Weld. Join. (2017) 1–8. doi:10.1080/13621718.2017.1355425.

[14] T. Itoi, A. Bin Mohamad, R. Suzuki, K. Okagawa, Microstructure evolution of a dissimilar junction interface between an Al sheet and a Ni-coated Cu sheet joined by magnetic pulse welding, Mater. Charact. 118 (2016) 142–148. doi:10.1016/j.matchar.2016.05.021.